

# Laser Diagnostics for Single Cycle Analysis of Crank Angle Resolved Length and Time Scales in Engine Combustion

R.R.Maly, G.Eberspach and W.Pfister

*Forschung und Technik  
Technische Physik - FVG/P  
Daimler-Benz AG  
Postfach 800 230  
D-7000 Stuttgart 80  
F.R.Germany*

## ABSTRACT

In developing predictive combustion models there is an urgent need for single cycle analysis of engine combustion. This is the only way to study in detail important issues e.g. the nature of cyclic variations in flow fields, mixing, flame propagation, heat transfer to walls etc.. Unfortunately the available diagnostic tools still work mostly pointwise and need many cycles for completing a consistent field measurement.

To overcome this drawback in conventional averaging and pointwise measuring techniques a crank angle resolved laser diagnostic has been developed for studying shape, structure and speed of engine flames along with a novel flame contour analysis for evaluating simultaneously time and length scales of flame wrinkling in individual engine cycles.

The single cycle diagnostic is based on movies of Mie scattered radiation from smoke particles taken in the fired chamber of an optically accessible engine (compression ratio: 10:1) allowing unobstructed access to all phases of the combustion process. To this end the radiation from a copper vapour laser (40 W, 3-20 kHz) is shaped into a thin (0.15 mm) 80 mm wide light sheet covering the full combustion process from BDC to TDC. Up to 60 images of the propagating flame (ignition to end of combustion) are taken at 3 crank angle intervals by a rotating mirror camera and are evaluated individually by a specially developed PC-based image processor.

Image evaluation provides a full quantitative description of all essential flame properties including time and length scales of flame wrinkling which are derived by auto- and cross correlations procedures. In addition essential parameters entering the BML-flamelet model are calculated.

In the paper the optically accessible research engine, the laser diagnostic setup and the image processing algorithms are presented in detail. Extensive data are given having been measured in a propane fueled engine for flames being close to extinction for engine speeds of 550, 1000 and 1500 rpm.

## EXPERIMENTAL SETUP

In order to provide unobstructed optical access throughout the full 720 degrees of crank angle (DCA) of an engine cycle a fully transparent

square piston engine has been built at Daimler Benz. The 4 side walls are made from optically ground quartz plates being firmly screwed together by 4 self-centering conical corner pieces and head and bottom plates, resp., made from mild steel. The quartz joints are made leakproof by a thin layer of soft plastic glue being temperature resistant up to 200 °C (Fig.1). The net blow-by is of the same order as in an oil lubricated production engine.

The square piston is built on top of an extension rod being bolted onto the piston of the single cylinder base engine (Hatz HE-673). The square piston is guided in the quartz section by a Turcon (Graphite/Teflon) plate and sealed by a precision-made single-piece seal made from the same material. This construction allows unlubricated operation of the transparent chamber for hours in the unfired mode and for bursts of 250 fired cycles at 10 minutes intervals. The lifetime of the seal allows operation of the engine for over a week. The compression ratio is 10:1 in the present case but may easily be changed by selecting different rod lengths and piston plates to simulate different engine designs (Fig.1).

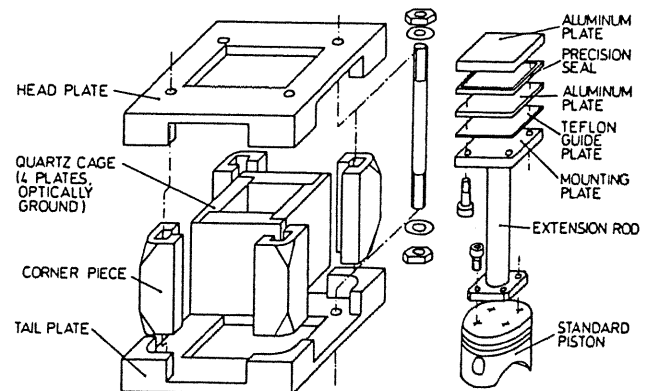


Fig.1 Details of the design of the transparent square combustion chamber and the square piston.

In order to avoid obscuration of 1 side window by the pushing rods of the valve train the rods were replaced by a hydraulic circuit passing the chamber at two side edges (Fig.2). The original valves and seats were retained but mounted in the left hand half of the head to allow insertion of an additional top window in the right hand side. In

this work, however, this space was used for mounting thermocouples, pressure transducer and spark plug (Fig.3).

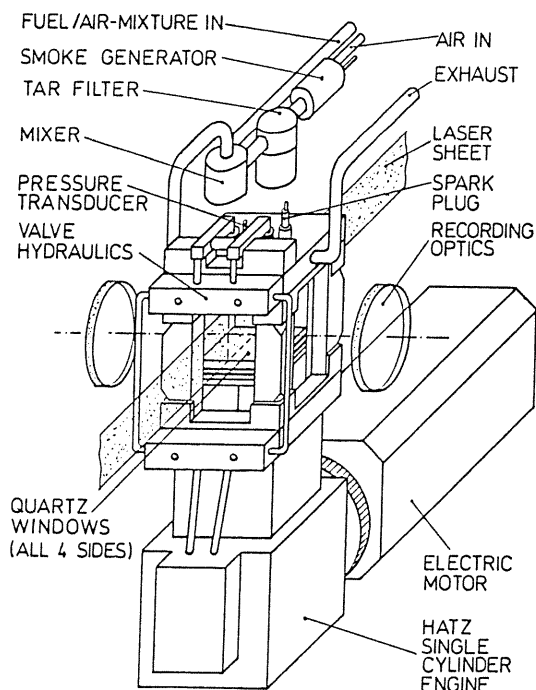


Fig.2 Square piston engine. Locations of hydraulic valve trains, smoke generator and laser sheet optics.

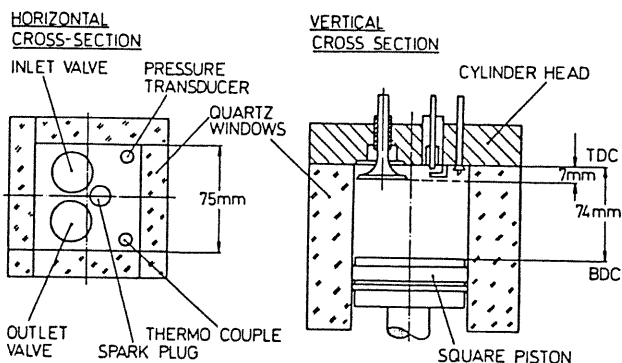


Fig.3 Details of the combustion chamber.

The engine was operated on propane/air mixtures being controlled by mass flow meters (1% accuracy). A fraction of the air (<10%) was seeded by cigarette smoke produced in a special smoke generator which was electrically started when engine conditions had stabilized (Fig.4).

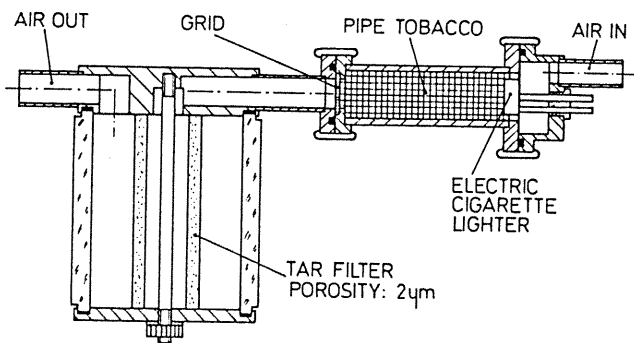


Fig.4 Cross-section of the cigarette smoke generator.

The leanness ratio (inverse of equivalence ratio) was determined from the mass fluxes and the oxygen content in the exhaust of the motored engine. The mixing system used is shown in Fig.5.

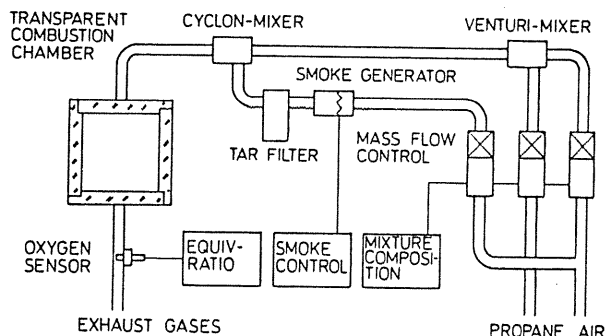


Fig.5 Gas mixing and seeding system.

The general characteristics of the optically accessible square piston engine are:

Piston area:	75x75 mm <sup>2</sup>
Piston rod:	112 mm
Stroke:	67 mm
Clearance height:	7 mm
Compression ratio:	10.2:1
Maximum speed:	2.500 1/min
Idle to full load, unfired and fired.	

**Laser Sheet Movies**

The radiation of a 40 W copper vapour laser is shaped into a thin (0.15 mm) 80 mm wide laser sheet illuminating the full vertical cross-section (BDC to TDC) of the optical engine at any instant. This sheet may be passed at any position being important for studying mixing or combustion processes. The Mie scattered signals from the smoke seeded propane/air charge are recorded at right angles using a rotating mirror framing camera. Details are given in Figures 6 and 7.

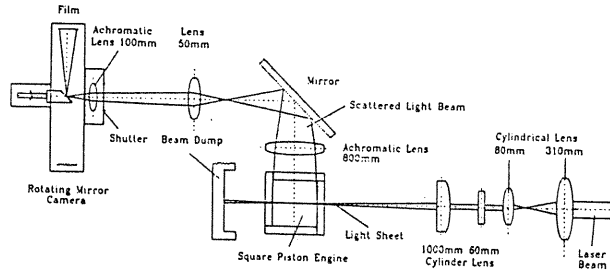


Fig.6 Optical setup for full view laser sheet filming of engine flames.

Except for requiring occasional cleaning of tar deposits the non-abrasive submicron smoke particles allow damage-free unlubricated motion of Turcon sealed pistons over quartz windows.

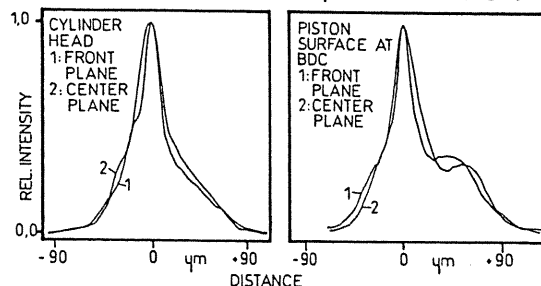


Fig.7 Measured laser sheet profiles in the transparent chamber.

For taking a laser sheet movie the engine is set to the desired operating conditions by monitoring the cylinder pressure and the IMEP first in the motored and then in the fired mode. When the engine has stabilized ignition is switched off and the smoke generator is turned on by the electric cigarette lighter delivering enough smoke for about 10 cycles (depending on engine load).

By a central electronic control the 3rd cycle is ignited and recorded on the camera. Since the smoke particles are burned the flame contour is resolved with a high contrast on 35 mm Kodak TMZ 5054 film /1/. During film exposure the normally free running laser is synchronized to the engine crank to produce a frame (size of negative: 17x17 mm<sup>2</sup>) every 3rd crank angle (maximum framing rate: 20 kHz). In such a way one cycle is recorded by 64 to 150 consecutive high resolution frames.

After developing the film the individual frames are read into a PC-based image processing system (512x512 pixels, dynamic: 8 bit, spatial resolution: 0.15 mm/pixel) and renormalized to the full grey level swing of 0-255. By thresholding at 90 a clear binary image of the flame is obtained (Fig.8) from which the left and right contour are derived by an edge detection scheme (Fig.9).

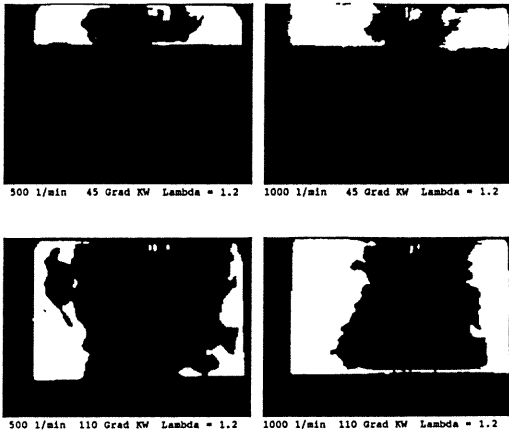


Fig.8 Laser sheet images at 45/110 DCA and 500/1000 rpm, respectively.

From these raw data the quantities: **burned area, wrinkling factor, mean flame radius and flame speed** are calculated by well known standard procedures. The fractal dimensions were checked but found to be useless for quantitative purposes due to excessive scatter being larger than corresponding variations in  $u'/S_L$  from 0-10.

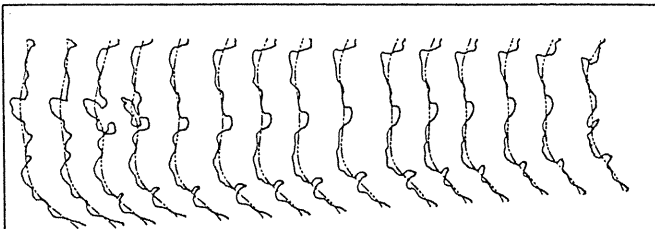


Fig.9 Consecutive flame contours, 114-156 DCA, 3 DCA intervals. Propane/air, Leanness ratio: 0.67, 1000 rpm, Ignition at TDC.

Quantitative flamelet data and length and time scales of flame wrinkling are calculated from flame contours after transformation into telegraph

signals. To this end a mean contour is calculated by low-pass Fourier filtration of the instantaneous flame contour. The cut-off length is chosen equal to half the instantaneous chamber height so that the mean contour represents the slowly varying, large structures due to mean motion only. The intersections of both curves define the burned/unburned segments of the telegraph signal (i.e. reaction progress variable  $c = 1$  or  $= 0$ ).

From this signal all relevant data for the BML flamelet model are calculated: **interval length, cosine value ( $\zeta_y$ ), crossing frequency, mean reaction progress variable ( $\bar{c}$ ), integral length and time scale of flame wrinkling ( $\hat{L}, T$ ).** Details may be found in the literature, therefore only the essential expressions are summarized here for convenience /2-5/:

BML reaction rate: 
$$w = \frac{\rho_r S_L^0 (P_0 + P_1 \frac{W_1}{W_2} + \dots) g z (1 - z)}{\sigma_y \hat{L}}$$

Intr. length scale: 
$$\hat{L} = \frac{1}{f(\Delta)} \int_0^{L_{max}} \frac{c(y)c(y+\Delta) - z^2}{z(1-z)} d\Delta$$

Intr. time scale: 
$$T_r = \int_{\tau}^{t_{dc}} R_{MN}(t) dt \quad R_{MN} = \prod_{j=M}^N R_j R_{j+1}$$

The **integral length (Bray) scale** of flame wrinkling is derived by integration of the autocorrelation of the telegraph function. From the cumulative product of the maxima of cross-correlations between adjacent contours the **integral time scale** is calculated. So the fate of a flame in a single cycle is fully characterized (Figs.10,11).

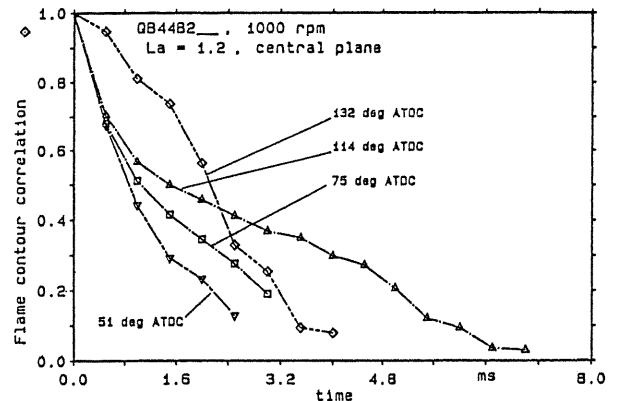


Fig.10 Autocorrelations for Fig.9.

In Figs.12-19 typical results are given for a volume quenched flame (propane/air, leanness ratio: 1.5, 1000 rpm, TDC ignition, 1/3 load).

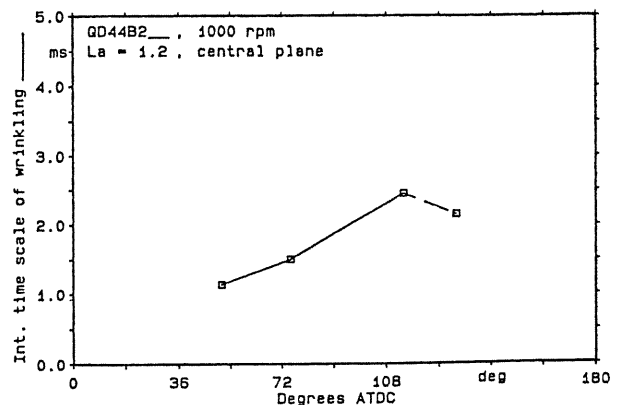


Fig.11 Calculated integral time scales.

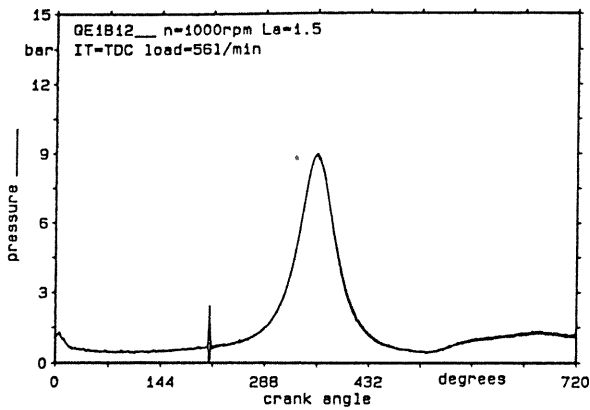


Fig.12 Motored and fired cylinder pressures for a volume quenched flame.

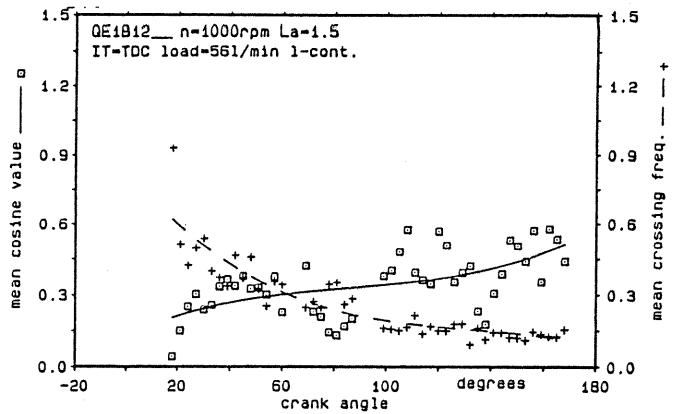


Fig.16 Left contour. Mean cosine values and crossing frequencies.

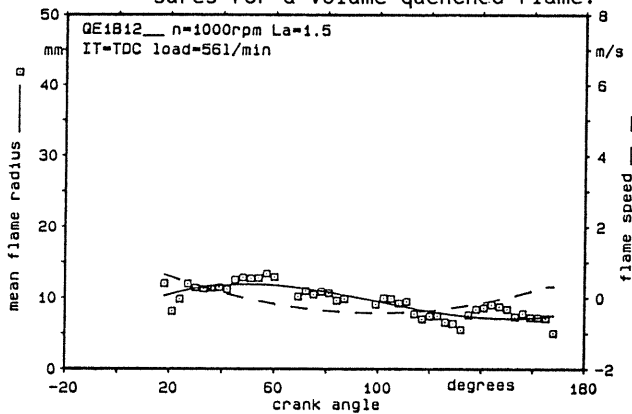


Fig.13 Flame radius and flame speed for a volume quenched flame.

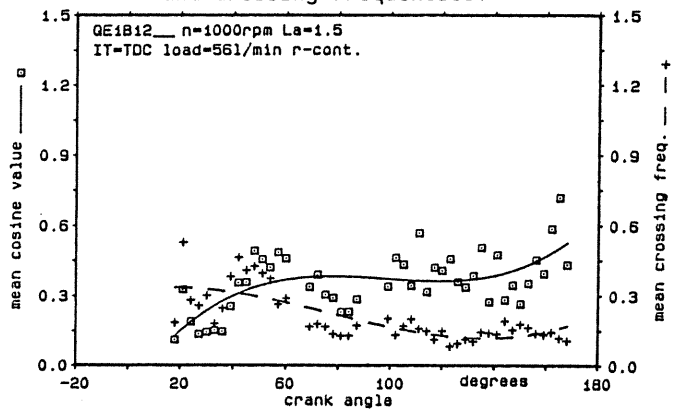


Fig.17 Right contour. Mean cosine values and crossing frequencies.

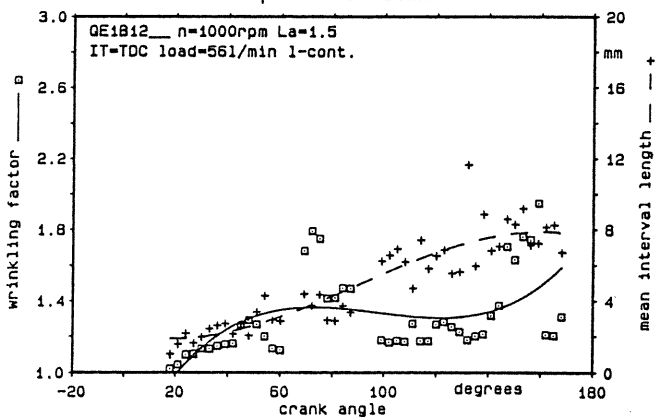


Fig.14 Left contour: Wrinkling factor and mean interval length.

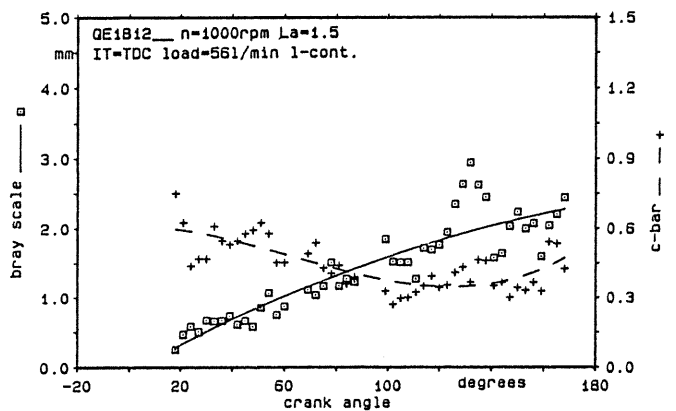


Fig.18 Left contour: Int. length (Bray) scale and mean progress variable.

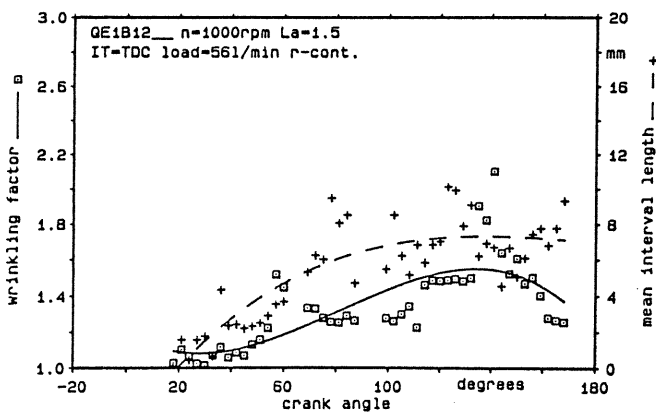


Fig.15 Right contour: Wrinkling factor and mean interval length.

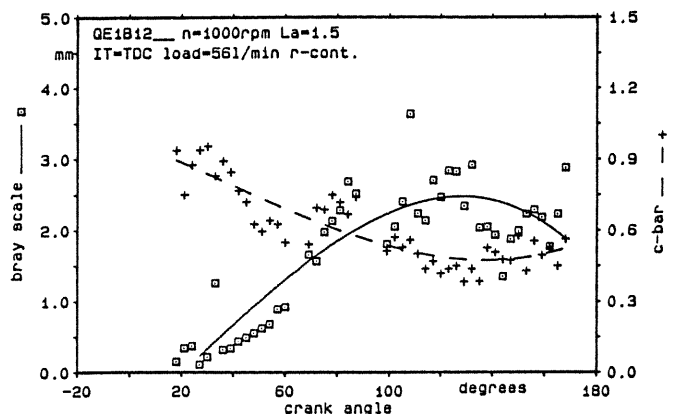


Fig.19 Right contour: Int. length (Bray) scale and mean progress variable.

RESULTS

Effect of Engine Speed

The variation of characteristic flame data are presented for volume quenched flames. In Fig.20 flame propagation is shown for 3 different but nominally identical cycles to illustrate the variations which can occur. Flames may be quenched very early (30 DCA) which later never recover, whereas at late quenching (90 DCA) the flame may start propagating again /6/.

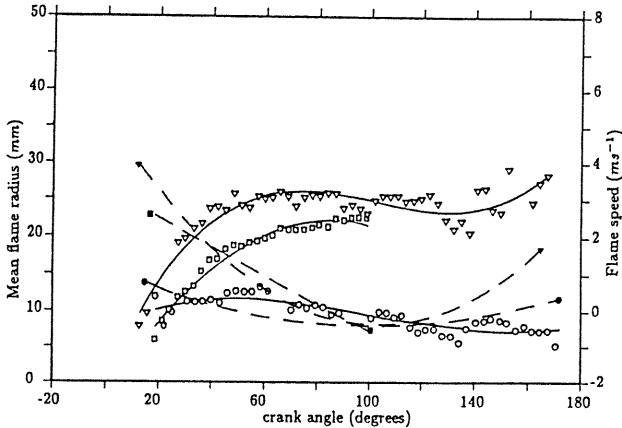


Fig.20 Nominally identical cycles at 1000 rpm, leanness ratio 1.5, TDC ign..

The number of crossings per mm flame contour depends very little (if at all) on engine speed, but hyperbolically on crank angle. This appears to be due to flame elongation and early decay of

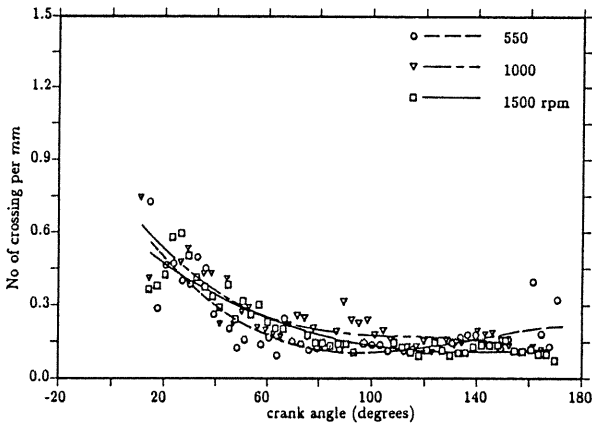


Fig.21 Measured crossing frequencies for 3 different engine speeds.

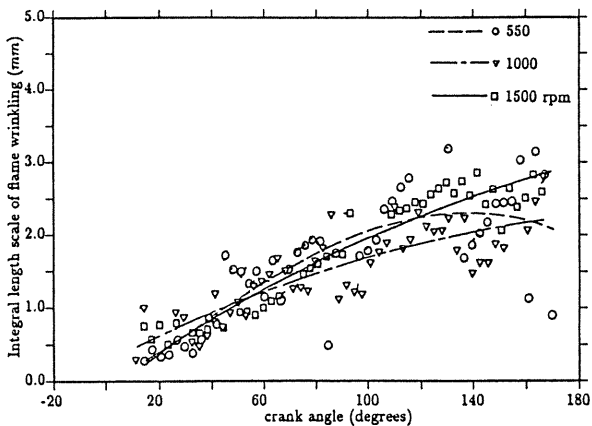


Fig.22 Integral length (Bray) scale for 3 different engine speeds.

small scale structures due to piston motion as shown in Fig.21.

The integral length scale of flame wrinkling (Bray scale) appears to depend very little on engine speed and hence on turbulence intensity (Fig.22). This is consistent with findings from other workers /7-9/ that the integral length scale of turbulence is usually of the order of 2 to 3 mm, independent of the actual engine cylinder configuration. Our experimental results is evidence therefore, that the integral length scale of flame wrinkling, as defined and evaluated above, is approximately equal to the integral length scale of the non-reacting turbulence field, even under conditions of engine combustion.

The integral time scales of flame wrinkling (T) are shown in Fig.23. Within the scatter T is proportional to  $(rpm)^{-1}$  as expected. It appears that the flame retains large structures over the entire cycle, and especially so for low turbulence levels, so that much of the history of a cycle is influenced by the shape of the flame kernel.

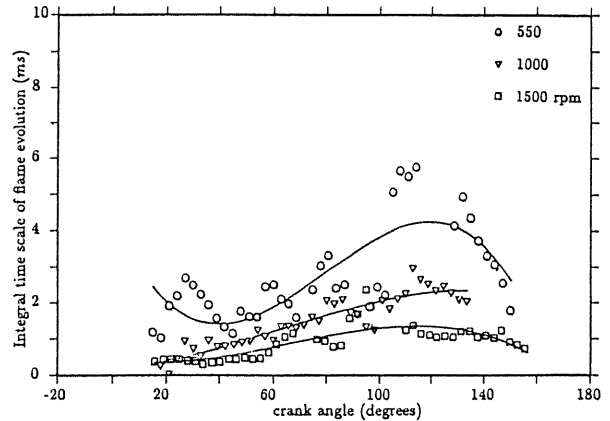


Fig.23 Integral time scale of flame wrinkling for 3 engine speeds.

The local mean direction cosine of the normal to the local flame front is shown in Fig.24, being =0 when the actual and mean contour are parallel and =1 when the contours are at right angles. The increase in direction cosine with crank angle implies therefore, that the flame is becoming more wrinkled during its history. This reinforces the view that an engine flame is constantly evolving over the entire cycle and represents a non-stationary and unique process from start to finish. Nevertheless, a mean value, as expected, is about 0.5.

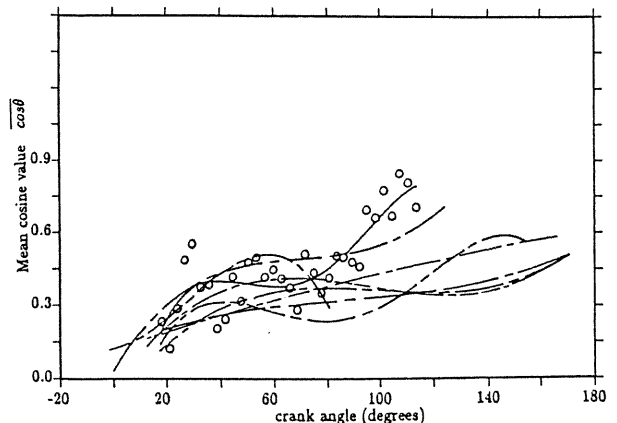


Fig.24 Mean direction cosine values for 6 different, nominally equal cycles.

### Comparison to BML-Calculations

Test calculations have been carried out with a modified version of the Bray-Moss-Libby flamelet model (BML) /10/. The modifications account for:

- instationary combustion
- flame quenching due to strain and transient flamelet heat loss arising from the rate of pressure changes in an engine
- full chemistry by incorporation of a strained flamelet library for propane/air combustion at realistic engine conditions
- gradient transport model for scalar fluxes
- cylindrical geometry.

Although the modelling work is still in progress the predictions are in good qualitative agreement with the laser sheet data obtained so far. Correct trends are predicted for flame propagation as function of stoichiometry, engine speed, ignition timing, strain rate, integral length scale, rate of pressure change and turbulence intensity.

As an example in Fig.25 the calculated flame development is compared with measured data. The results are given for 2 different reaction progress variables. The agreement is within the scatter of the experimental data.

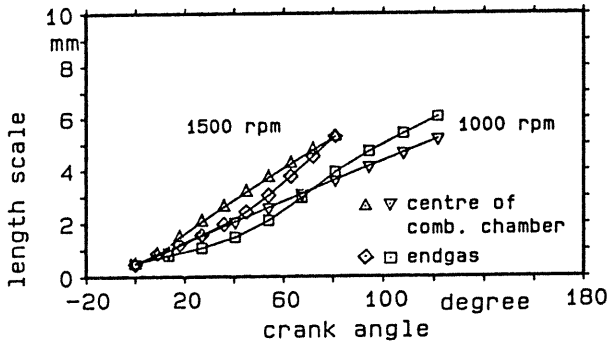


Fig.25 Calculated and measured flame evolution. Propane/air, leanness ratio: 1.5, TDC ignition, 1/3 load.

In Fig.26 the predicted change of the integral length scale with crank angle is presented. There is a slight overprediction for large crank angles which is assumed to be due to the fact that the calculation is still made in 2D. Nevertheless there is a very good general agreement regarding dependencies of speed, crank angle and location in the chamber.

The results indicate that the reduction in burning rate in the square piston engine is due not to strain but to transient heat losses induced by the rate of pressure change.

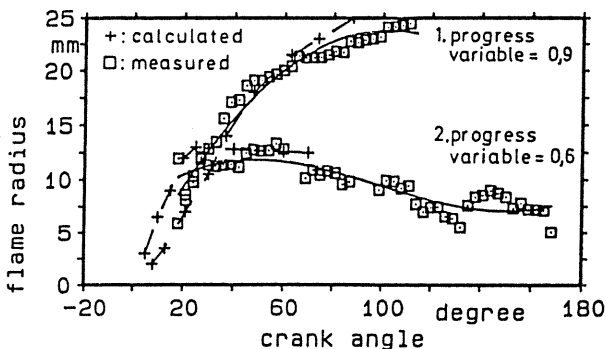


Fig.26 Calculated effect of engine speed on the integral length scale.

### CONCLUSION

A laser sheet diagnostic has been presented offering a quantitative analysis of flame propagation in single engine cycles. The diagnostic incorporates a fully transparent square piston engine and a Mie scattering technique for taking high resolution laser sheet movies of the full chamber size throughout complete engine cycles.

The movies are evaluated by specially developed image processing software with regards to all relevant flamelet data of the BML model. In addition cycle resolved time and length scales are evaluated being in good agreement with literature data and predictions from a modified BML flamelet code designed to model engine combustion.

Extensive experimental data from a single cycle analysis of volume quenched engine flames at 550, 1000 and 1500 rpm are presented with special emphasis on the BML parameters:

- burned area
- flame radius
- interval length
- crossing frequency
- integr. length scale
- wrinkling factor
- flame speed
- cosine value
- progress variable
- integr. time scale

### ACKNOWLEDGEMENT

This work was supported by Daimler Benz and the Commission of the European Community (EN3E-0056-D)

### REFERENCES

1. Ziegler, G.F.W., Zettlitz, A., Meinhardt, P., Herweg, R., Maly, R.R. and Pfister, W., "Cycle-Resolved Two-Dimensional Flame and Flow Visualization in a Spark-Ignition Engine", SAE paper, 881634, 1988.
2. Bray, K.N.C. and Libby, P.A., "Passage Times and Flamelet Crossing Frequencies in Premixed Turbulent Combustion", Combust. Sci. Technol., Vol 47, pp. 253, 1986.
3. Chew, T.C., "PhD Thesis", University of Cambridge, 1988.
4. Chew, T.C., Britter, R.E. and Bray, K.N.C., "Laser Tomography of Premixed Turbulent Bunsen Flames", Combustion and Flame, Vol. 75, pp. 165, 1989.
5. Maly, R.R., Bray, K.N.C. and Chew, T.C., "An Integral Time Scale of Evolution for Non-Stationary Turbulent Premixed Flames", Combust. Sci. and Technol., Vol. 66, pp. 139, 1989.
6. Bray, K.N.C., Chew, T.C. and Maly, R.R., "Quantitative Evaluation of Length and Time Scales of Turbulent Engine Combustion from 2D Laser Sheets, Proc. 7th Symp. Turb. Shear Flow, Aug. 21-23, Stanford University, 1989.
7. Witze, P.O., "A Critical Comparison of Hot-Wire Anemometry and Laser Doppler Velocimetry for I.C. Engine Applications", SAE paper 800132, 1988.
8. Fraser, R.A. and Bracco, F.V., "Cycle-Resolved LDV Integral Length Scale Measurements in an I.C. Engine", SAE paper 880381, 1988.
9. Dinsdale, S., Roughton, A. and Collins, N., "Length Scale and Turbulence Intensity Measurements in a Motored I.C. Engine, SAE paper 880380, 1988.
10. Maly, R.R., "Improved Otto-Cycle by Enhancing the Final Phase of Combustion", Final Report, Commission European Community, Contract EN3E-0056-D, 1989.